ISSN 1063-7834, Physics of the Solid State, 2006, Vol. 48, No. 2, pp. 224–228. © Pleiades Publishing, Inc., 2006.
Original Russian Text © D.V. Gritsenko, S.S. Shaĭmeev, V.V. Atuchin, T.I. Grigor'eva, L.D. Pokrovskiĭ, O.P. Pchelyakov, V.A. Gritsenko, A.L. Aseev, V.G. Lifshits, 2006, published in Fizika Tverdogo Tela, 2006, Vol. 48, No. 2, pp. 210–213.

SEMICONDUCTORS AND DIELECTRICS

Two-Band Conduction in TiO_2

D. V. Gritsenko*, S. S. Shaĭmeev*, V. V. Atuchin*, T. I. Grigor'eva*, L. D. Pokrovskiĭ*, O. P. Pchelyakov*, V. A. Gritsenko*, A. L. Aseev*, and V. G. Lifshits**

** Institute of Semiconductor Physics, Siberian Division, Russian Academy of Sciences, pr. Akademika Lavrent'eva 13, Novosibirsk, 630090 Russia*

e-mail: grits@isp.nsc.ru

*** Institute of Automatics and Control Processes, Far East Division, Russian Academy of Sciences, Vladivostok, 690041 Russia*

Received May 12, 2005

Abstract—The contribution of electrons and holes to the electrical conduction of titanium dioxide TiO_2 in the $Si/TiO_2/Al$ structure is determined in experiments on the injection of minority carriers from *n*-type and *p*-type silicon layers. It is established that both electrons and holes contribute to electrical conduction of the titanium dioxide layer in the $Si/TiO_2/Al$ structure; i.e., the electrical conduction of titanium dioxide has a two-band nature.

PACS numbers:

DOI: 10.1134/S1063783406020053

1. INTRODUCTION

Scaling of metal–insulator–silicon devices is accompanied by a shortening of the channel and a decrease in the thickness of the gate dielectric. Over the past four decades, thermal silicon dioxide SiO_2 has been used as the primary gate-dielectric material in field-effect devices. A decrease in the thickness of the silicon dioxide layer to 10–15 Å leads to an unacceptably high intensity of the leakage current. A radical approach to the reduction of the leakage current through a gate dielectric consists in replacing silicon dioxide with so-called alternative dielectrics (dielectrics with a high permittivity, i.e., high-*k* dielectrics). The use of alternative dielectrics makes it possible to increase the physical thickness of the dielectric layer and, consequently, to suppress the tunnel current [1, 2]. Another application of alternative dielectrics is associated with their use in charge storage capacitors of random-access memory cells [2]. In recent years, it has been proposed to use alternative dielectrics for the purpose of increasing the operational speed of Flash memory devices [3]. Titanium dioxide TiO_2 is one of the most promising materials for use as an alternative dielectric. There exist four phases of titanium dioxide, namely, amorphous titanium dioxide, rutile, anatase, and brookite [4]. Titanium dioxide possesses a high permittivity ($\varepsilon \approx 80$) with a band gap $E_g \approx 3.2$–3.8 eV [5, 6]. In general, the electrical conduction in dielectrics is provided by electrons and holes. The sign of the charge carriers in semiconductors is determined using either the Hall effect or thermopower. These techniques are not applicable to dielectrics because of the low concentration of mobile carriers. The purpose of this work was to determine the contribution made by electrons and holes to the electrical conduction of dielectric titanium dioxide layers in a $Si/TiO_2/Al$ structure prepared through oxidation of metallic titanium evaporated on a silicon substrate.

2. SYNTHESIS OF TiO_2 LAYERS

The $Si/TiO_2/Al$ structures were synthesized on *n*-Si(100) and *p*-Si(100) plates with an electrical resistivity of ≈10 Ω cm. Titanium dioxide layers were prepared through high-temperature oxidation of metallic titanium films. Thermal evaporation of titanium onto a silicon substrate heated to a temperature of 100°C was performed from a tungsten vessel under vacuum at a residual pressure of 6.7×10^{-4} Pa. The thickness of the metal film was checked against the electrical resistance measured on a special quartz substrate immediately in the process of evaporation. The dependence of the electrical resistance of the titanium films on the film thickness in the range 50–350 Å was preliminarily measured using ellipsometry. As is known [7, 8], surface oxidation of titanium films can lead to a deficit of diffused oxygen in the bulk of the oxidized layer with the formation of TiO_{2-x} suboxides whose chemical composition significantly deviates from stoichiometry. In order to suppress this effect, the formation of titanium oxide was performed in two stages. At each stage, after the deposition of a metal film 200 ± 50 Å thick, the samples were subjected to oxidation in air in a platinum vessel at a temperature of 750°C for 7 h. According to the ellipsometric measurements, the total thickness of the titanium dioxide layers varied in the range from 600 to

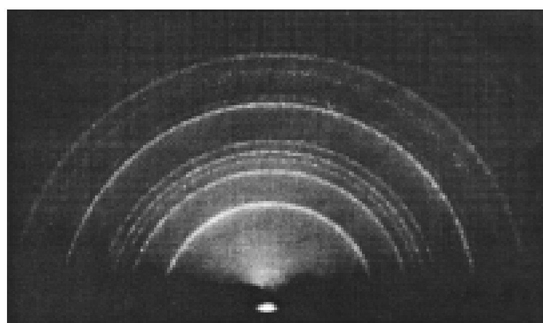

Fig. 1. RHEED pattern (65 kV) of the surface of the titanium dioxide film prepared through titanium oxidation at a temperature of 750°C.

1000 Å. The contact pads suitable for electrical measurements were formed by thermal evaporation of aluminum films ~2000 Å thick through a mask under vacuum at a residual pressure of 6.7×10^{-4} Pa and at a substrate temperature of 150°C.

After each stage of oxidation, the phase composition of the layers was controlled by recording the reflection high-energy electron diffraction (RHEED) patterns. A typical RHEED pattern is shown in Fig. 1. In all four cases, the surface phase was identified as polycrystalline rutile. The RHEED patterns were indexed using the tabulated parameters for rutile. The results obtained are presented in the table.

3. ELECTRICAL MEASUREMENTS

The current–voltage and capacitance–voltage (at a frequency of 100 kHz) characteristics were measured at room temperature. The illumination was performed with the use of a tungsten lamp. Figure 2 shows the current–voltage characteristics of the p-Si/TiO_2/Al structure measured for two polarities of the potential applied to the metal: (i) in the enhancement mode (with a negative potential across the aluminum layer) and (ii) in the depletion mode (with a positive potential across the aluminum layer). In the depletion mode, when the potential across the aluminum layer in the dark is positive, the electric current reaches saturation and depends only weakly on the voltage. Under illumination, the intensity of the electric current increases. The saturation of the electric current in the depletion mode is caused by the injection of the minority charge carriers (in our case, electrons) from silicon into the dielectric. In the enhancement mode, when the potential across the metal

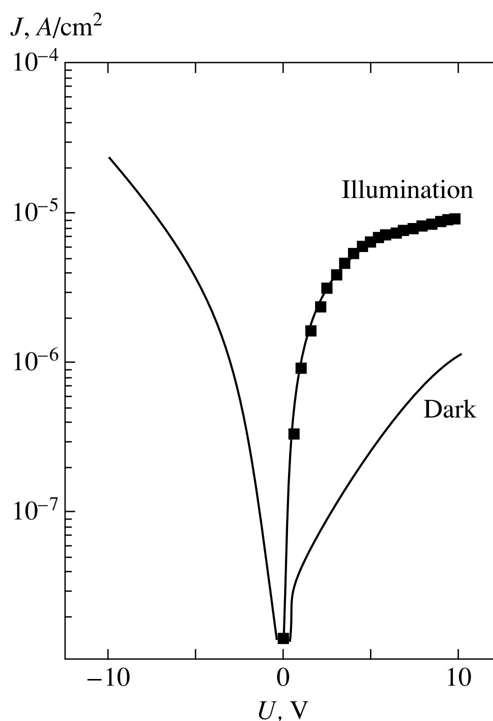

Fig. 2. Current–voltage characteristics for the p-Si/TiO_2/Al structure in the depletion and enhancement modes (solid lines). Points represent the current–voltage characteristic measured in the depletion mode under illumination. The thickness of the titanium dioxide layer is 800 Å.

Interplanar distances d_{exp} and intensities I_{exp} of the spectral lines for the surface phase of titanium dioxide prepared through titanium oxidation at a temperature of 750°C

d_{exp}, Å	I_{exp}	d^*_{tab}, Å	I^*_{tab}	hkl
3.29	Very strong	3.248	100	110
2.51	Strong	2.487	50	101
2.31	Weak	2.297	8	200
2.21	Medium-weak	2.188	25	111
2.07	″	2.054	10	210
1.70	Strong	1.687	60	211
1.64	Very weak	1.624	20	220

* *Powder Diffraction File*: *Inorganic Phases*, Joint Committee for Powder Diffraction Standards, International Center for Diffraction Data, 1601 Park Line, Swarthmore, Pennsylvania, 19081, United States, Data Cards, set 21-1276.

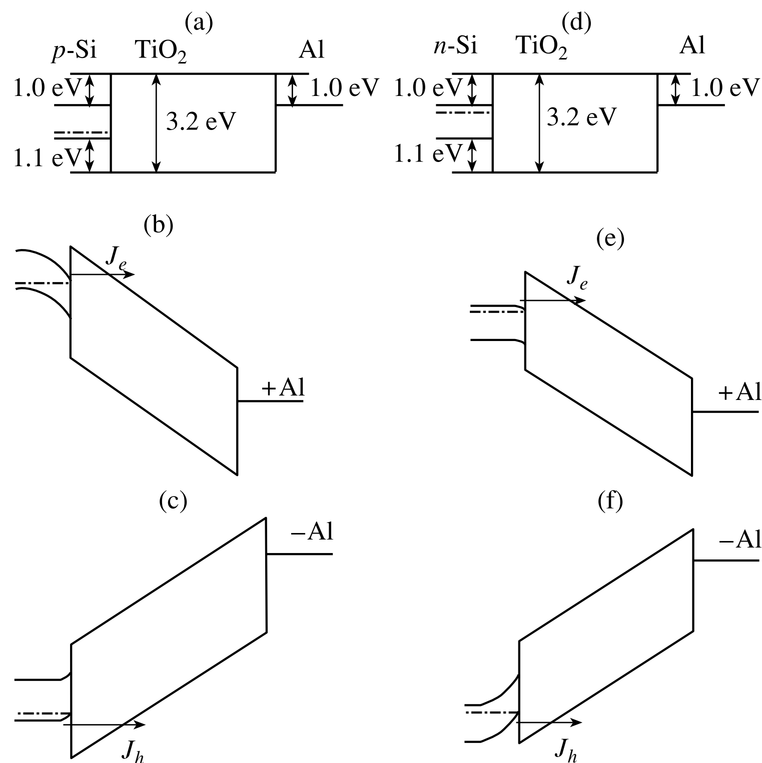

Fig. 3. Schematic energy diagrams for (a–c) p-Si/TiO_2/Al and (d–f) n-Si/TiO_2/Al structures (a, d) with no external applied voltage, (b, f) in the depletion mode, and (c, e) in the enhancement mode.

layer is negative, the intensity of the electric current increases exponentially with an increase in the potential. The illumination does not affect the intensity of the electric current. In this case, virtually all the applied voltage drops across the dielectric layer.

The schematic energy diagrams for the Si/TiO_2/Al structures with p-type and n-type silicon layers are depicted in Figs. 3a–3f. The band gap for TiO_2 is assumed to be equal to 3.2 eV [5], and the barrier height for electrons at the Si/TiO_2 interface is taken to be 1.0 eV [9]. In this case, the band gap for silicon is 1.12 eV and the barrier height for holes at the Si/TiO_2 interface is equal to 1.1 eV. The Fermi level for aluminum coincides with the conduction band edge for silicon. Consequently, the barrier height for electrons at the Al/TiO_2 interface is equal to 1.0 eV. Figure 3 shows the schematic energy diagrams for the p-Si/TiO_2/Al and n-Si/TiO_2/Al structures with positive (Figs. 3b, 3e) and negative (Figs. 3c, 3f) potentials applied to the metal.

In the depletion mode, the voltage applied to the p-Si/TiO_2/Al structure is distributed between the dielectric layer and the nonequilibrium depletion layer (see Fig. 3b). This can be explained by the fact that the injection current of minority carriers (electrons) is comparable to the rate of their generation in silicon. The illumination brings about an increase in the rate of generation of minority carriers, a decrease in the thickness of the depletion layer, a decrease in the voltage drop across the depletion layer, an increase in the voltage drop across the dielectric layer, and, consequently, an increase in the electrical conductivity of the dielectric. Thus, the current–voltage characteristics of the p-Si/TiO_2/Al structure in the depletion mode (Fig. 2) indicate that, for the case of a positive potential across the aluminum layer, the dominant contribution to the electrical conduction of the titanium dioxide layer is made by the injection of electrons from silicon (Figs. 3b, 3e). The flow of holes from the dielectric into silicon is negligible as compared to the counterflow of electrons from silicon into the dielectric. When there is a negative potential across the metal layer in the enhancement mode (Fig. 3c), all the applied voltage drops across the dielectric layer. It is reasonable to assume that, in this case, electrical conduction in the dielectric material is also provided by electrons injected from silicon, because the barrier heights for electrons at the Si/TiO_2 and Al/TiO_2 interfaces are equal (Figs. 3a, 3d).

A similar behavior of the current–voltage characteristics is observed for the n-Si/TiO_2/Al structure (Fig. 4). With a positive potential across the metal layer in the enhancement mode, all the applied voltage drops across the dielectric layer (Fig. 3e). It can be assumed that, as in the p-Si/TiO_2/Al structure, the charge transfer in the dielectric layer in the n-Si/TiO_2/Al structure occurs through electrons injected from silicon (Fig. 3e). For

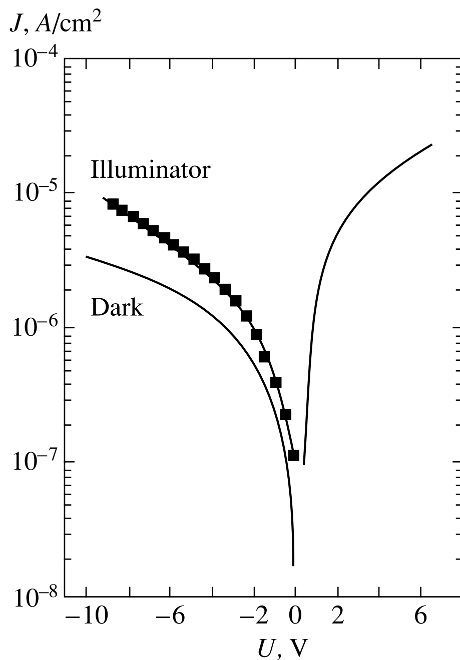

Fig. 4. Current–voltage characteristics for the n-Si/TiO_2/Al structure in the depletion and enhancement modes (solid lines). Points represent the current–voltage characteristic measured in the depletion mode under illumination. The thickness of the titanium dioxide layer is 900 Å.

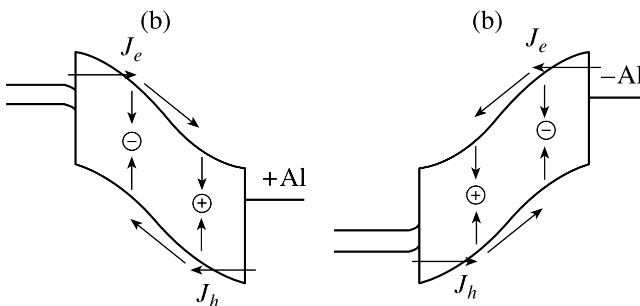

Fig. 5. Schematic diagram illustrating the passage of the electric current through the Si/TiO_2/Al structure with (a) positive and (b) negative potentials across the metal. In the depletion mode, the rate of generation of minority carriers is assumed to be higher than the rate of their injection into the dielectric material.

the case of a negative potential applied to the metal in the depletion mode, the current–voltage characteristics reach saturation (Fig. 4). The illumination leads to an increase in the intensity of the electric current. This means that a nonequilibrium depletion layer develops in silicon due to the injection of holes from silicon into the dielectric (Fig. 3f). As follows from the data obtained for n-Si near the Si/TiO_2 interface, the electric current is provided by holes injected from silicon into the dielectric material.

It is reasonable to assume that, in the p-Si/TiO_2/Al structure with a negative potential applied to the metal, the charge transfer in the dielectric layer is also provided by holes injected from silicon (Fig. 3c). In the general case, electrons are injected into the dielectric from the negatively biased electrode whereas holes are injected into the dielectric from the positively biased electrode. There is experimental evidence that titanium dioxide contains traps [10–13]. Figure 5 illustrates the two-band mechanism of the passage of the electric current provided by electrons and holes in the Si/TiO_2/Al structure for two polarities of the potential applied to the metal. According to this model, titanium dioxide contains both electron and hole traps, which act as recombination centers. Let us consider in greater detail the passage of the electric current through the structure when the polarity of the potential applied to the metal is positive (Fig. 5a). In this case, electrons are injected from silicon into titanium dioxide, in which they are trapped. Part of the electrons are ionized from the traps either according to the Frenkel mechanism or through the multiphonon mechanism [13, 14]. Then, conduction electrons recombine with holes trapped in the vicinity of the anode (metal). Holes are injected from the positively biased anode into the valence band of the dielectric and trapped and then recombine with free electrons. Part of the hole traps are ionized, and the released holes move toward silicon and recombine with localized electrons. This model explains the development of the nonequilibrium depletion layer in n-type and p-type silicon semiconductors in terms of the injection of minority carriers into the dielectric. A similar situation takes place when a negative potential is applied to the metal (Fig. 5b). The proposed model is similar to the model of an electric current flowing in silicon nitride [14–16].

ACKNOWLEDGMENTS

This work was performed within the framework of the Integration Project of the Siberian Division of the Russian Academy of Sciences, project no. 116.

REFERENCES

1. A. I. Kingon, J.-P. Maria, and S. K. Streiffer, Nature (London) **406**, 1032 (2000).
2. G. D. Wilk, R. M. Wallace, and J. M. Anthony, J. Appl. Phys. **89**, 5243 (2001).
3. V. A. Gritsenko, K. A. Nasyrov, Yu. N. Novikov, A. L. Aseev, S. Y. Yoon, J.-W. Lee, E.-H. Lee, and C. W. Kim, Solid-State Electron. **47** (10), 1651 (2003).
4. S.-D. Mo and W. Y. Ching, Phys. Rev. B: Condens. Matter **51**, 13 023 (1995).
5. V. Mikhelashvili and G. Eisenstein, J. Appl. Phys. **89**, 3256 (2001).
6. S. A. Campbell and D. C. Kim, IBM J. Res. Dev. **43**, 383 (1999).

7. Bryce S. Richards, S. Raymond Richards, Matthew B. Boreland, and David N. Jamieson, J. Vac. Sci. Technol., A **22** (2), 339 (2004).
8. Gang He, Qi Fang, Liqiang Zhu, Mao Liu, and Lide Zhang, Chem. Phys. Lett. **395**, 259 (2004).
9. S. A. Campbell, D. C. Gilmer, X.-C. Wang, M.-T. Hsieh, H.-S. Kim, W. L. Glasdfelter, and J. Yan, IEEE Trans. Electron Devices **44**, 104 (1997).
10. J. W. Halley, M. T. Michalewicz, and N. Ti, Phys. Rev. B: Condens. Matter **41** (10), 165 (1990).
11. F. Montoncello, M. C. Carotta, B. Cavicchi, M. Ferroni, A. Giberti, V. Guidi, C. Malagu, G. Martinelli, and F. Meinardi, J. Appl. Phys. **94**, 1501 (2003).
12. G. K. Dalapati, S. Chatterjee, S. K. Samantu, S. K. Nandu, P. K. Bose, S. Varma, S. Patil, and C. K. Maiti, Solid-State Electron. **47**, 1793 (2003).
13. K. A. Nasyrov, V. A. Gritsenko, Yu. N. Novikov, E.-H. Lee, S. Y. Yoon, and C. W. Kim, J. Appl. Phys. **96**, 4293 (2004).
14. V. A. Gritsenko, E. E. Meerson, and Yu. N. Morokov, Phys. Rev. B: Condens. Matter **57**, R2081 (1997).
15. A. S. Ginovker, V. A. Gritsenko, and S. P. Sinitsa, Phys. Status Solidi B **26**, 489 (1974).
16. K. A. Nasyrov, Yu. N. Novikov, V. A. Gritsenko, S. Yu. Yoon, and C. W. Kim, Pis'ma Zh. Éksp. Teor. Fiz. **77**, 455 (2003) [JETP Lett. **77**, 385 (2003)].

Translated by V. Artyukhov

SPELL: OK